Mechanics & Industry **27**, 34 (2026)

https://doi.org/10.1051/meca/2026032

Mechanics & Industry

Available online at:
www.mechanics-industry.org

ORIGINAL ARTICLE

OPEN ACCESS

Brittle-ductile synergistic compressive behavior of the material-extruded hybrid structure with an embedded rhombicuboctahedron core in additive manufacturing: a preliminary study

Donghyeon Kim, Bogyeom Choi, Jaerin Kim, Jeongin Lee, and Seong Je Park*

School of Mechanical Engineering, Gyeongsang National University, 501 Jinju-daero, Jinju-si, Gyeongsangnam-do 52828, Republic of Korea

Received: 11 June 2026 / Accepted: 29 June 2026

Abstract. In this study, a hybrid structure with an embedded rhombicuboctahedral core was fabricated using a material extrusion process, and its compressive behavior was investigated. Polylactic acid (PLA) was used as a stiff internal core, while thermoplastic copolyester (TPC) served as a compliant matrix. The hybrid structure exhibited a specific compressive strength and mass-normalized energy absorption approximately 1.46 times and 1.74–1.86 times higher than that of the TPC-based cubic structure. While the TPC structure showed a typical plateau behavior associated with progressive collapse, the hybrid structure demonstrated a higher initial stiffness and a continuously increasing stress response with noticeable stress fluctuations due to the sequential yielding of the PLA core. This behavior reflects a brittle–ductile synergistic effect, where the TPC matrix enables energy absorption and the PLA core enhances load-bearing capacity. These findings highlight the potential of multi-material additive manufacturing for designing mechanically efficient hybrid structures.

Keywords: Additive manufacturing / material extrusion / rhombicuboctahedron / hybrid structure / specific compressive strength

1 Introduction

With recent advances in material extrusion (MEX), multi-material MEX systems capable of simultaneously depositing materials with distinct mechanical properties within a single build process have become increasingly widespread [1–3]. This capability enables the fabrication of hybrid structures combining materials with distinct mechanical properties, offering new opportunities for tailoring structural performance beyond conventional single-material designs [4,5]. Most previous studies on additively manufactured structures have focused on single-material systems or periodically repeated lattice architectures. In single-material structures, the overall mechanical response is primarily governed by the intrinsic properties of the constituent material and the structural geometry. For example, Hanks et al. reported that the mechanical properties of additively manufactured lattice structures vary significantly with unit-cell topology, highlighting the importance of architectural design in determining structural performance [6]. Furthermore, Li et al. reviewed a wide range of additively manufactured lattice structures and concluded that their mechanical response is governed by factors such as topology, relative density, material system, and loading conditions [7]. Although these studies demonstrated the effectiveness of geometric optimization and material selection, the mechanical response of single-material lattice structures remains fundamentally governed by the intrinsic properties of the constituent material. Consequently, it is challenging to simultaneously achieve multiple functional requirements, such as high load-bearing capacity, controlled deformation, and efficient energy absorption, beyond the inherent limitations of a single material system [8–11].

To address this limitation, hybrid structures integrating materials with contrasting mechanical responses have attracted increasing attention [12,13]. Harris et al. reported that hybrid lattice-walled honeycomb structures exhibited superior specific strength and energy absorption efficiency compared with conventional lattice structures [14]. Similarly, Zhang et al. demonstrated that hybrid lattice structures combining different unit-cell topologies achieved enhanced energy absorption while maintaining

* e-mail: seongje.park@gnu.ac.kr

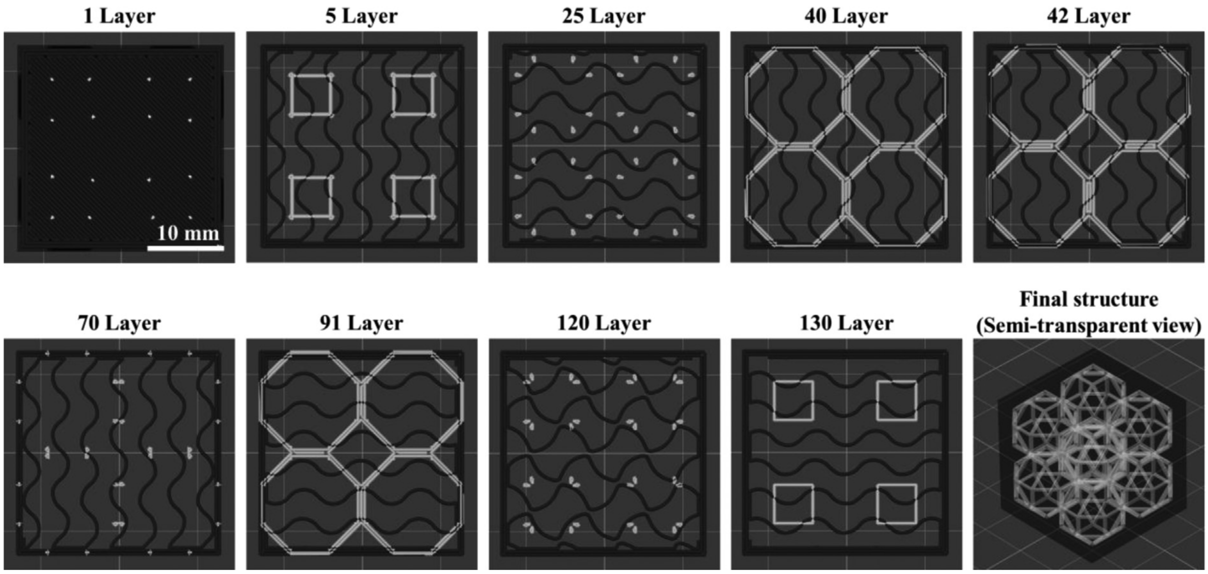

Fig. 1. Selected layers of the proposed PLA–TPC hybrid structure (PLA: white, TPC: black).

comparable stiffness [15]. More recently, Abbas et al. reported that multi-material lattice structures enabled tailored deformation behavior and improved mechanical performance through the synergistic interaction of constituent materials [16]. In particular, embedding a relatively stiff internal topology within a compliant matrix has emerged as an effective strategy for achieving a synergistic response under compressive loading [17–19]. In such systems, the compliant phase accommodates initial deformation and mitigates stress concentration, while the stiff phase enhances load-bearing capacity and structural stability [20,21]. Among various internal topologies, the rhombicuboctahedron is of interest due to its high geometric symmetry, which can promote uniform load distribution and reduced directional dependence in mechanical response, making it suitable as an embedded internal core [22–24].

In this study, the compressive behavior of PLA-based rhombicuboctahedral structures fabricated under different MEX processing conditions was first investigated to establish baseline mechanical performance. Based on the optimized conditions, a hybrid structure was designed by embedding the PLA-based rhombicuboctahedral core within a thermoplastic copolyester (TPC) matrix using a multi-material MEX process. The compressive behavior of the hybrid structure was then evaluated and compared with that of a TPC-based cubic structure. The results reveal a brittle–ductile synergistic effect, leading to enhanced specific compressive strength and controlled deformation behavior.

2 Methodology

An MEX system (H2D, Bambu Lab, China) was used to fabricate all specimens in this study. The MEX is equipped with a dual nozzle, enabling the deposition of different thermoplastic filaments within a single build process. A commercial PLA filament (HS PLA, Hanil Industry Co., Ltd., Republic of Korea) was employed as the relatively stiff phase, while a TPC (TPC 55D, Hanil Industry Co., Ltd., Republic of Korea) was used as the compliant phase. To investigate the compressive strength of the PLA-based rhombicuboctahedral topology, intended as the internal core, specimens were fabricated under different MEX processing conditions. Specifically, the nozzle temperature (190–230°C) and the layer thickness (0.10, 0.15, and 0.20 mm) were selected as key process parameters. The nozzle temperature was selected due to its strong correlation with interfacial adhesion and overall mechanical strength in MEX processes, while the layer thickness was varied considering its influence on build efficiency [25–27]. A nozzle diameter of 0.4 mm, a fill density of 100%, a nozzle speed of 250 mm/s, a bed temperature of 80°C, and a raster angle of ±45° were used. The rhombicuboctahedral structure was designed by arranging two-unit cells (one-unit cell size: 13 mm) along each of the three orthogonal directions, resulting in a specimen size of 26 × 26 × 26 mm. In the case of the TPC cube with a volume of 26 × 26 × 26 mm^3, a layer thickness of 0.10 mm, a nozzle temperature of 270°C, a fill density of 15%, a nozzle speed of 250 mm/s, a bed temperature of 80°C, and a raster angle of 0/90° with a gyroid pattern (the top and bottom three layers were configured at 100% infill with a raster angle of ±45°) were used. For the hybrid structure, the PLA rhombicuboctahedral core was embedded within the TPC cubic matrix using the dual-nozzle MEX system, as shown in Figure 1. Figure 1 presents characteristic layer configurations extracted from the fabrication process to highlight the evolution of the embedded rhombicuboctahedral core. Since the hybrid structure consisted of a total of 260 layers and the upper half was geometrically symmetric to the lower half, only the first 130 layers are presented for clarity. The fabrication process began with the deposition of the TPC matrix at layer 1, followed by the gradual formation of the internal PLA rhombicuboctahedral core.

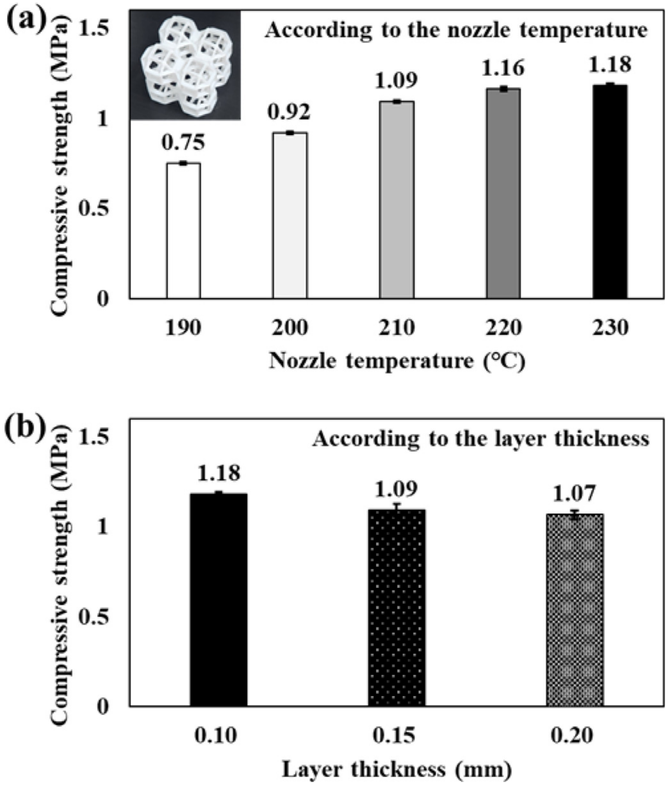

Fig. 2. Compressive strength of MEXed PLA-based rhombicuboctahedron according to the (a) nozzle temperature and (b) layer thickness.

All specimens were designed using Tinkercad (Autodesk Inc., USA). To evaluate the compressive properties of the PLA-based rhombicuboctahedral structures, TPC cubic structures, and the corresponding hybrid structures, compression tests were conducted. The tests were performed using a universal testing machine (AGX-10kNVD, Shimadzu, Japan). All specimens were compressed at a constant crosshead speed of 5 mm/min until the applied load reached 10 kN. For each experimental condition, three specimens were tested to ensure reproducibility, and the compressive strength, specific compressive strength, and mass-normalized energy absorption are displayed as average values with corresponding standard deviations. In particular, to further evaluate the mass-normalized energy absorption (MEA) capability of the structures, the area under the specific compressive stress–strain curve was calculated at strains of 40% (MEA_{40}), 50% (MEA_{50}), 60% (MEA_{60}), and 70% (MEA_{70}) as follows:

$$\int_0^{\varepsilon} \sigma_s d\varepsilon$$

where σ_s is the specific compressive stress (MPa/g), and ε is the compressive strain corresponding to 0.4, 0.5, 0.6, and 0.7 for MEA40, MEA50, MEA60, and MEA70, respectively. The strain values were converted from percentage to dimensionless strain prior to integration.

3 Results and discussion

3.1 Compressive behavior of PLA-based rhombicuboctahedron according to the nozzle temperature and layer thickness

Since material-extruded (MEXed) thermoplastic materials are highly sensitive to thermal conditions, the influence of nozzle temperature was first examined, as it strongly affects interlayer bonding. Subsequently, the effect of layer thickness was investigated [28].

Figure 2a shows the compressive strength of the PLA-based rhombicuboctahedral structures as a function of nozzle temperature (layer thickness: 0.10 mm). As the nozzle temperature increased from 190 to 230°C, the compressive strength steadily increased from 0.75 to 1.18 MPa, corresponding to an improvement of approximately 57%. In particular, the compressive strength increased from 0.75 MPa at 190°C to 1.09 MPa at 210°C, indicating a significant enhancement in the low-to-intermediate temperature range. Beyond 210°C, the rate of increase became relatively moderate, reaching 1.16 MPa at 220°C and 1.18 MPa at 230°C. This nonlinear trend was well described by a second-order polynomial relationship, where y represents the compressive strength (MPa) and x denotes the nozzle temperature (°C): $y = -0.0289x^2 + 0.2839x + 0.4875$ ($R^2 = 0.9952$), indicating an excellent correlation between nozzle temperature and compressive strength. The negative quadratic term reflects the diminishing rate of strength increase at higher nozzle temperatures.

Figure 2b presents the compressive strength of the PLA-based rhombicuboctahedral structures as a function of layer thickness. Compared with the nozzle temperature, the influence of layer thickness on compressive strength was relatively less pronounced. As the layer thickness increased from 0.10 to 0.20 mm, the compressive strength slightly decreased from 1.18 to 1.07 MPa, corresponding to a reduction of approximately 9%. Specifically, the compressive strength decreased from 1.18 MPa at 0.10 mm to 1.09 MPa at 0.15 mm and further to 1.07 MPa at 0.20 mm. This decreasing trend can be attributed to the reduced interlayer bonding quality at larger layer thicknesses, where fewer interfaces are formed and the contact area between adjacent filaments becomes less effective for stress transfer [29–31]. The relationship between layer thickness and compressive strength was well described by a second-order polynomial function, where y represents the compressive strength (MPa) and x denotes the layer thickness (mm): $y = 0.0329x^2 - 0.1897x + 1.3382$ ($R^2 = 1$). The positive quadratic term suggests a mild curvature, although the overall trend remains decreasing within the investigated range.

3.2 Comparison of compressive behavior between TPC-based cubic and PLA–TPC hybrid structures

Based on the optimized processing conditions for the PLA-based rhombicuboctahedral structure identified in Section 3.1 (nozzle temperature of 230°C and layer thickness of 0.10 mm), a hybrid structure was fabricated

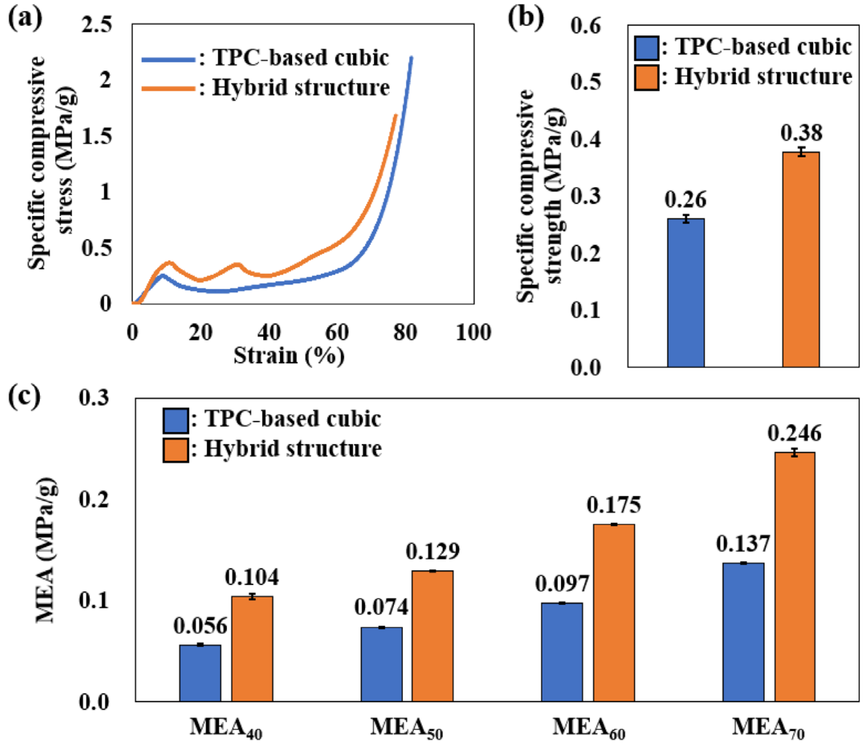

Fig. 3. (a) Specific compressive stress–strain curve, (b) specific compressive strength, and (c) MEA of TPC-based cubic and hybrid structure (TPC-based cubic + PLA-based rhombicuboctahedron).

by embedding the PLA core within a TPC-based cubic matrix. The compressive behavior of the hybrid structure was compared with that of the TPC-based cubic structure to evaluate the effect of the embedded internal topology.

Figure 3a shows the specific compressive stress–strain curves of both structures. The TPC-based cubic structure exhibited a low initial stiffness followed by an extended plateau region, where the stress remained relatively constant over a wide strain range. In contrast, the hybrid structure demonstrated a higher initial stiffness and a more pronounced stress increase with increasing strain. Unlike the TPC-based cubic structure, which exhibited a relatively smooth plateau region, the hybrid structure showed noticeable fluctuations in the stress–strain response, characterized by repeated stress rises and drops during compression. This serrated behavior is attributed to the subsequent yielding or collapse of the embedded PLA-based rhombicuboctahedral core [32,33]. Especially at the initial stage, the compliant TPC matrix deformed first, accommodating the applied load and reducing stress concentration. As the deformation progressed, the embedded PLA rhombicuboctahedral core gradually engaged, contributing to load support and resisting further deformation. This synergistic interaction between the compliant matrix and the stiff internal core led to a more controlled and progressive deformation process.

Figure 3b presents the specific compressive strength of the TPC-based cubic and the hybrid structure. The hybrid structure exhibited a specific compressive strength approximately 1.46 times higher than that of the TPC-based cubic structure. This enhancement can be attributed to the presence of the PLA-based rhombicuboctahedral core, which provides additional load-bearing capability while maintaining a relatively low overall density.

Figure 3c presents the MEA_{40}, MEA_{50}, MEA_{60}, and MEA_{70} of the TPC-based cubic and hybrid structures at strains of 40%, 50%, 60%, and 70%, respectively. The strain values were converted from percentage to dimensionless strain (0.4, 0.5, 0.6, and 0.7, respectively) prior to integration. At all strain levels, the hybrid structure exhibited higher MEA values than the TPC-based cubic structure. Specifically, the hybrid structure exhibited higher MEA values than the TPC-based cubic structure, increasing from 0.056 to 0.104 MPa/g (1.86 times higher) at 40% strain, from 0.074 to 0.129 MPa/g (1.74 times higher) at 50% strain, from 0.097 to 0.175 MPa/g (1.80 times higher) at 60% strain, and from 0.137 to 0.246 MPa/g (1.80 times higher) at 70% strain. These results indicate that the incorporation of the PLA-based rhombicuboctahedral core consistently improved the MEA capability throughout the compression process.

The sequential deformation behavior during compression is illustrated in Figure 4, where the TPC-based cubic structure and the hybrid structure are denoted by blue and orange outlines, respectively. For the TPC-based cubic structure, representative deformation states are shown at strains of 14% (post-yield region) and 50% (prior to densification). At a strain of 14%, the structure entered the plateau region immediately after yielding. At a strain of 50%, a substantial reduction in specimen height was

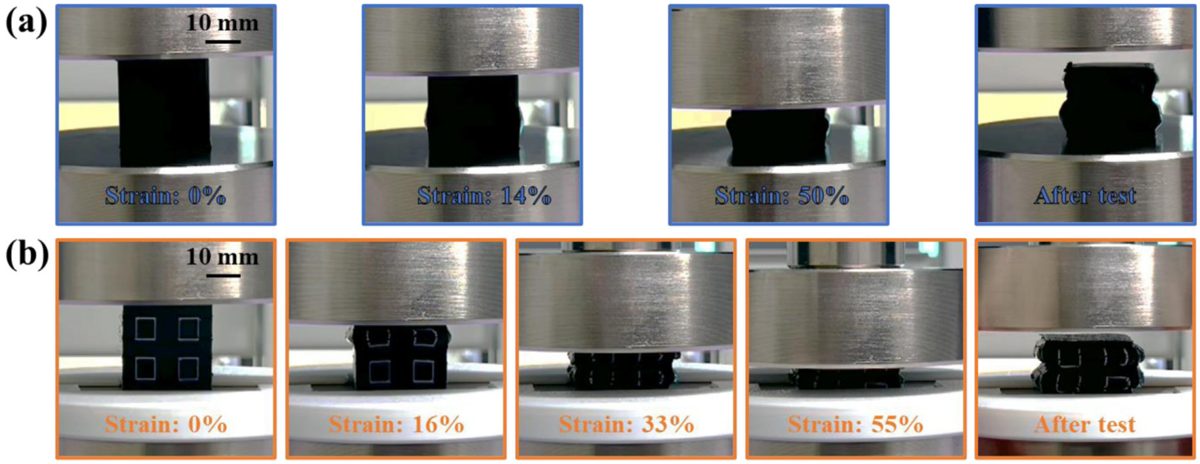

Fig. 4. Sequential deformation behavior of (a) TPC-based cubic and (b) hybrid structure (TPC-based cubic + PLA-based rhombicuboctahedron).

observed prior to densification. In contrast, for the hybrid structure, the deformation states corresponding to the post-first-yield and post-second-yield regions are illustrated at strains of 16% and 33%, respectively. At strains of 16% and 33%, progressive compression of the hybrid structure was observed following the first and second yield events, respectively. In addition, a representative deformation state prior to densification is presented at a strain of around 55%, where a further reduction in specimen height was observed. After unloading, the TPC-based cubic structure exhibited a noticeable tendency for shape recovery due to its inherent elasticity. In the hybrid structure, partial recovery was also observed, primarily attributed to the elastic response of the TPC matrix, although the overall deformation remained partially irreversible due to the plastic deformation of the embedded PLA core. Overall, the hybrid structure demonstrated a brittle–ductile synergistic behavior, where the ductile TPC matrix mitigates stress concentration and delays failure, while the relatively stiff PLA core enhances load-bearing capacity and structural stability. This combination results in improved compressive performance and energy absorption characteristics compared with the single-material TPC structure.

To further investigate the failure mechanism of the structures after compression, the specimens were sectioned along the upper region, and their internal morphologies were examined, as shown in Figure 5. The TPC-based cubic structure maintained a relatively continuous internal architecture after compression, not fracture. In contrast, the hybrid structure exhibited fragmentation of the embedded PLA rhombicuboctahedral core, while the surrounding TPC matrix remained largely intact. These observations indicate that the enhanced compressive response of the hybrid structure was primarily associated with the progressive fracture of the PLA core, which contributed to load-bearing capacity and energy dissipation during compression.

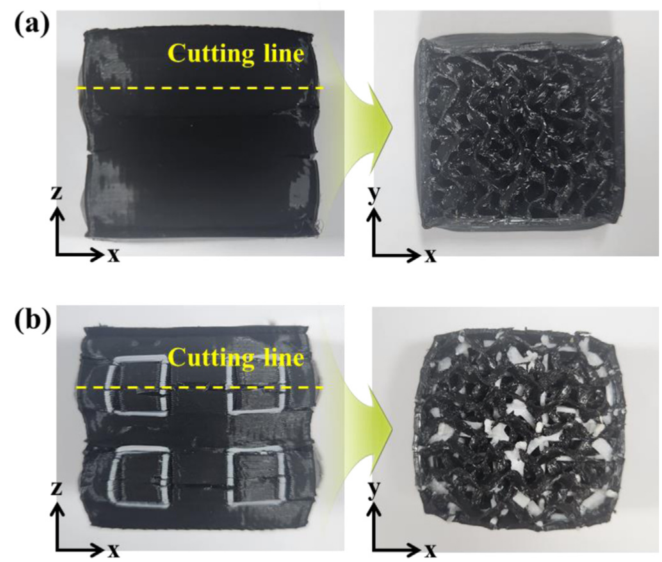

Fig. 5. Cross-sectional images of the compressed specimens after the compressive test: (a) TPC-based cubic structure and (b) hybrid structure (TPC-based cubic + PLA-based rhombicuboctahedron).

3.3 Conceptual applications of the proposed hybrid structure

Although the present study focused on the compressive behavior of the proposed hybrid structure, its mechanical characteristics suggest potential applicability in various protective engineering systems. As illustrated in Figure 6, three representative application concepts are proposed, including drone electronics protection, electric vehicle (EV) component protection, and sensor protection. In these applications, the protected components are positioned within the hybrid structure, while the embedded

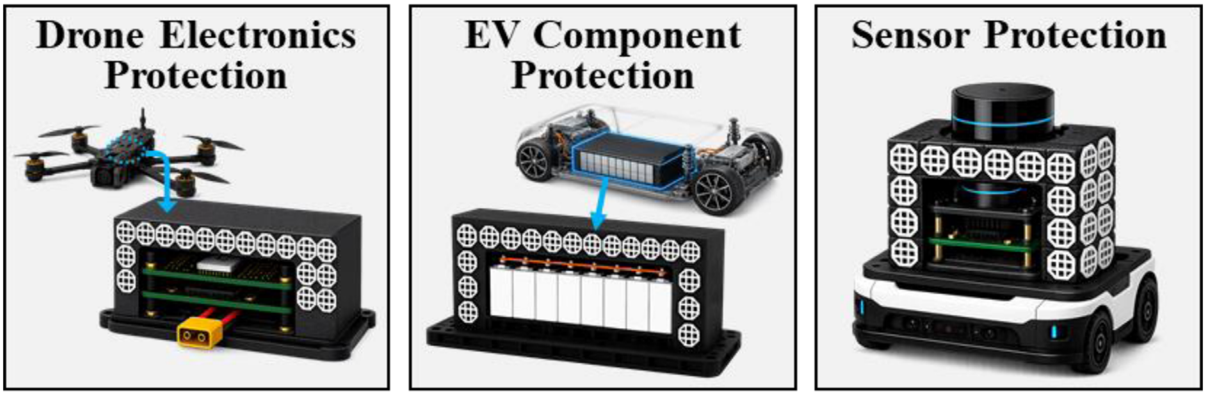

Fig. 6. Potential engineering applications of the proposed PLA–TPC hybrid structure in protective systems for drone electronics, EV components, and sensors.

rhombicuboctahedral core serves as a sacrificial energy-absorbing element. When external loads or impact events occur, the compliant TPC matrix initially accommodates deformation, followed by the progressive collapse and fracture of the rhombicuboctahedral core. Through this mechanism, a portion of the impact energy can be dissipated by the hybrid structure itself, thereby reducing the load transferred to the protected internal components. For drone electronics protection, electronic modules are frequently exposed to impact loads during landing, transportation, or accidental collisions. The proposed hybrid structure can serve as an energy-absorbing protective housing, where the compliant TPC matrix accommodates deformation while the embedded PLA rhombicuboctahedral core provides structural support and impact resistance. In EV applications, battery modules and electronic components require lightweight protective structures capable of mitigating mechanical damage caused by external loading. The combination of high specific compressive strength and progressive deformation behavior observed in the hybrid structure may provide a lightweight alternative for protective pads or housing components. For sensor protection systems, maintaining sensor integrity under mechanical loading is critical for reliable operation. The proposed hybrid structure may function as a protective enclosure that simultaneously offers load-bearing capability and energy absorption, thereby reducing the risk of sensor damage while minimizing additional weight. However, it should be noted that the hybrid structure exhibited substantially reduced shape recoverability compared with the TPC-based cubic structure, as shown in Figure 4, due to the irreversible deformation of the embedded PLA core. Therefore, the proposed hybrid structure is more suitable for single-use sacrificial protection applications, where impact energy absorption and protection of critical internal components are prioritized over structural reusability. Nevertheless, the observed brittle–ductile synergistic behavior and enhanced specific compressive strength indicate that the proposed hybrid structure has considerable potential for future protective engineering applications requiring both lightweight design and impact mitigation.

4 Conclusion

In this study, the compressive behavior of a hybrid structure with an embedded PLA-based rhombicuboctahedral core was investigated using a multi-material MEX process. The compressive strength of the PLA-based rhombicuboctahedral structure was significantly influenced by processing conditions, with the optimal condition identified as a nozzle temperature of 230°C and a layer thickness of 0.10 mm. The hybrid structure exhibited a specific compressive strength and MEA approximately 1.46 times and 1.74–1.86 times higher than that of the TPC-based cubic structure, respectively. While the TPC structure showed a typical plateau behavior associated with progressive collapse, the hybrid structure demonstrated a higher initial stiffness and a continuously increasing stress response with stress fluctuations due to the sequential yielding of the PLA core. Furthermore, deformation analysis revealed a distinct deformation sequence in the hybrid structure, where the compliant TPC matrix deformed first, followed by the gradual engagement of the PLA core. This interaction resulted in a brittle–ductile synergistic behavior, combining energy absorption and load-bearing capabilities. Notably, the hybrid structure exhibited a compressive strength (3.12 MPa) substantially higher than that of both the PLA-based rhombicuboctahedral structure (1.18 MPa) and the TPC-based cubic structure (1.78 MPa), suggesting that the enhanced mechanical performance is associated with the combined contribution of the embedded PLA core and the surrounding TPC matrix. These results demonstrate that embedding functionally designed internal topologies via multi-material additive manufacturing is an effective strategy for enhancing compressive performance and controlling deformation behavior in structural applications. However, the present study was not specifically designed to quantitatively separate the individual effects of material combination and structural topology. Therefore, future studies involving additional control structures are required to systematically distinguish and quantify their respective contributions.

Acknowledgments

The conceptual illustrations shown in Figure 4 were generated using OpenAI ChatGPT and are provided for visualization purposes only. They do not represent experimentally validated products or engineering designs.

Funding

This research received no external funding.

Conflicts of interest

The authors declare that they have no known competing financial interests or personal relationships that could have appeared to influence the work reported in this paper.

Data availability statement

Data will be made available on request.

Author contribution statement

Donghyeon Kim: Writing–original draft, Investigation, Conceptualization, and Methodology.
Bogyeom Choi: Data curation, Formal analysis, and Investigation.
Jaerin Kim: Methodology and Conceptualization.
Jeongin Lee: Visualization and Formal analysis.
Seong Je Park: Conceptualization, Resources, Funding acquisition, Visualization, and Writing–review & editing.

References

[1] M. Rajeshirke, I. Fidan, V. Naikwadi, S. Alkunte, A. Gupta, M. Mohammadizadeh, Material extrusion—based multi-material 3D printing: a holistic review of recent advances, Int J Adv Manuf Technol **139**, 149–174 (2025)

[2] M.A. Jafor, N. Sayah, D.E. Smith, G. Stano, T.J. Fleck, Systematic evaluation of adhesion and fracture toughness in multi-material fused deposition material extrusion, Materials **17**, 3953 (2024)

[3] A. Nazir, O. Gokcekaya, K. Md Masum Billah, O. Ertugrul, J. Jiang, J. Sun, S. Hussain, Multi-material additive manufacturing: a systematic review of design, properties, applications, challenges, and 3D printing of materials and cellular metamaterials, Mater. Des. **226**, 111661 (2023)

[4] L. Farràs-Tasias, J. Topart, S. Panier, F.A. Gilabert, F.H. Marchesini, Enhancing interfacial toughness of 3D printed bi-material polymers via mechanical interlocking and engineered fiber bridging, Addit. Manuf. **100**, 104684 (2025)

[5] O. Ulkir, S. Ersoy, Hybrid experimental–machine learning study on the mechanical behavior of polymer composite structures fabricated via FDM, Polymers **17**, 2012 (2025)

[6] B. Hanks, J. Berthel, M. Frecker, T.W. Simpson, Mechanical properties of additively manufactured metal lattice structures: data review and design interface, Addit. Manuf. **35**, 101301 (2020)

[7] Y. Li, D. Jiang, R. Zhao, X. Wang, L. Wang, L.-C. Zhang, High mechanical performance of lattice structures fabricated by additive manufacturing, Metals **14**, 1165 (2024)

[8] C. Neff, N. Hopkinson, N.B. Crane, Experimental and analytical investigation of mechanical behavior of laser-sintered diamond-lattice structures, Addit. Manuf. **22**, 807–816 (2018)

[9] C. Tian, Y. Wang, H. Fan, X. Li, Research progress of additively manufactured metallic lattice structures, Micromachines **16**, 1418 (2025)

[10] Y. Zhang, N. Li, Data-driven design for additive manufacturing of energy absorption lattice structures with variable density, Mater. Des. **259**, 114761 (2025)

[11] J. Yang, H. Liu, G. Cai, H. Jin, Additive manufacturing and influencing factors of lattice structures: a review, Materials (Basel) **18**, 1397 (2025)

[12] R. Raj, M. Jiyalal Prajapati, J.-T. Tsai, A. Kumar, J.-Y. Jeng, Design and additive manufacturing of novel hybrid lattice metamaterial for enhanced energy absorption and structural stability, Mater. Des. **245**, 113268 (2024)

[13] A. Ghimire, P.-Y. Chen, Mechanical properties of additively manufactured multi-material stiff-soft interfaces: Guidelines to manufacture complex interface composites with tunable properties, Mater. Des. **238**, 112677 (2024)

[14] J.A. Harris, R.E. Winter, G.J. McShane, Impact response of additively manufactured metallic hybrid lattice materials, Int. J. Impact Eng. **104** 177–191 (2017)

[15] J. Zhang, H. Huang, G. Liu, H. Zong, C. Zhang, Stiffness and energy absorption of additive manufactured hybrid lattice structures, Virtual Phys. Prototyp. **16**, 428–443 (2021)

[16] M. Abbas, K. Azher, A. Nazir, Multi-material integration for multifunctional enhancement of additively manufactured cubic strut and plate-lattice structures, Sci. Rep. **16**, 15308 (2026)

[17] H. Kiratli, E. Salamci, Additive manufacturing of lattice structures with hybrid unit cell: a study on manufacturability and strength, Proc. Inst. Mech. Eng. Part C J. Mech. Eng. Sci. **240**, 1467–1477 (2026)

[18] Q. Song, A. Singh, N. Karathanasopoulos, Hybrid manufacturing and mechanics of architected interpenetrating phase composites: review and perspectives, Virtual Phys. Prototyp. **20**, e2505992 (2025)

[19] R. Freund, H. Watschke, J. Heubach, T. Vietor, Determination of influencing factors on interface strength of additively manufactured multi-material parts by material extrusion, Appl. Sci. **9**, 1782 (2019)

[20] J. Zhang, H. Huang, G. Liu, H. Zong, C. Zhang, Stiffness and energy absorption of additive manufactured hybrid lattice structures, Virtual Phys. Prototyp. **16**, 428–443 (2021)

[21] X. Yang, Y. Gong, L. Zhao, J. Zhang, N. Hu, Compressive mechanical properties of layer hybrid lattice structures fabricated by laser powder bed fusion technique, J. Mater. Res. Technol. **22**, 1800–1811 (2023)

[22] J. Kim, D. Kim, J. Lee, S.J. Park, Geometric and compressive characteristics of the additive-manufactured rhombicuboctahedron structure and its application, Materials **19**, 619 (2026)

[23] R. Hedayati, M. Sadighi, M. Mohammadi-Aghdam, A.A. Zadpoor, Mechanics of additively manufactured porous biomaterials based on the rhombicuboctahedron unit cell, J. Mech. Behav. Biomed. Mater. **53**, 272–294 (2016)

[24] P. Nogueira, P. Lopes, L. Oliveira, J.L. Alves, J.P.G. Magrinho, A.M. de Deus, M.F. Vaz, M.B. Silva, Evaluation of lattice structures for medical implants: a study on the mechanical properties of various unit cell types, Metals **14**, 780 (2024)

[25] M.S. Sutopa, T. Sultan, E.H. Rozin, X. Xu, J. Gardan, C. Cetinkaya, Monitoring for the effects of extruder nozzle temperature on the micro-mechanical properties of 3D printed phononic artifacts, J. Manuf. Process. **98**, 337–350 (2023)

[26] R. Spurgeon, S.R. Begum, M. Saravana Kumar, M. Vasumathi, A.A. Adediran, Effect of nozzle temperature and infill patterns on enhancing crashworthiness performance of 3D printed glass fibre reinforced PLA parts, Sci. Rep. **15**, 34161 (2025)

[27] K. Shergill, Y. Chen, S. Bull, An investigation into the layer thickness effect on the mechanical properties of additively manufactured polymers: PLA and ABS, Int. J. Adv. Manuf. Technol. **126**, 3651–3665 (2023)

[28] F. Rivera-López, M.M.L. Pavón, E.C. Correa, M.H. Molina, Effects of nozzle temperature on mechanical properties of polylactic acid specimens fabricated by fused deposition modeling, Polymers (Basel) **16**, 1867 (2024)

[29] C. Tang, J. Liu, Y. Yang, Y. Liu, S. Jiang, W. Hao, Effect of process parameters on mechanical properties of 3D printed PLA lattice structures, Compos. Part C Open Access **3**, 100076 (2020)

[30] M.S. Kumar, M.U. Farooq, N.S. Ross, C.-H. Yang, V. Kavimani, A.A. Adediran, Achieving effective interlayer bonding of PLA parts during the material extrusion process with enhanced mechanical properties, Sci. Rep. **13**, 6800 (2023)

[31] A. Özen, G. Ganzosch, C. Völlmecke, D. Auhl, Characterization and multiscale modeling of the mechanical properties for FDM-printed copper-reinforced PLA composites, Polymers **14**, 3512 (2022)

[32] S. Li, M. Hu, L. Xiao, W. Song, Compressive properties and collapse behavior of additively-manufactured layered-hybrid lattice structures under static and dynamic loadings, Thin-Walled Structures **157**, 107153 (2020)

[33] M. Al Rifaie, A. Mian, R. Srinivasan, Compression behavior of three-dimensional printed polymer lattice structures, Proc. Inst. Mech. Eng. Part L J. Mater. Des. Appl. **233**, 1574–1584 (2019)

Cite this article as: D. Kim, B. Choi, J. Kim, J. Lee, S.J. Park, Brittle-ductile synergistic compressive behavior of the material-extruded hybrid structure with an embedded rhombicuboctahedron core in additive manufacturing: a preliminary study, Mechanics & Industry **27**, 34 (2026), https://doi.org/10.1051/meca/2026032